



# EIS studies of a corrosion inhibitor behavior under multiphase flow conditions

Y. Chen\*, T. Hong, M. Gopal, W.P. Jepson

*NSF I/UCRC, Corrosion in Multiphase Systems Center, Department of Chemical Engineering, Ohio University, Athens, OH 45701, USA*

Received 2 March 1999; accepted 6 September 1999

---

## Abstract

EIS studies of an imidazoline-based inhibitor under multiphase flow conditions were conducted in a large diameter flow loop system. The Warburg diffusion parameter,  $b_f = \sigma\omega^{-1/2}$  was used to qualitatively analyze inhibitor films formed on the metal surface. Experimental results show that the inhibitor films become less porous with increase in exposure time and inhibitor concentration. Inhibition performance of the corrosion inhibitor is reduced in slug flow at high rate of turbulence and bubble impact. This study demonstrates that EIS is an effective technique to investigate the inhibition performance of corrosion inhibitors in turbulent flow conditions. © 2000 Elsevier Science Ltd. All rights reserved.

*Keywords:* EIS; Low alloy steel; Acid inhibitor

---

## 1. Introduction

The organic corrosion inhibition is the most effective means of protecting the severely internal corrosion of carbon steel pipelines for oil product transportation. Imidazoline-based inhibitors are well known to have a high inhibition ability in acidic media, hence they are widely used to minimize carbon dioxide induced corrosion by oil and gas industries. The oil products from the wells are required

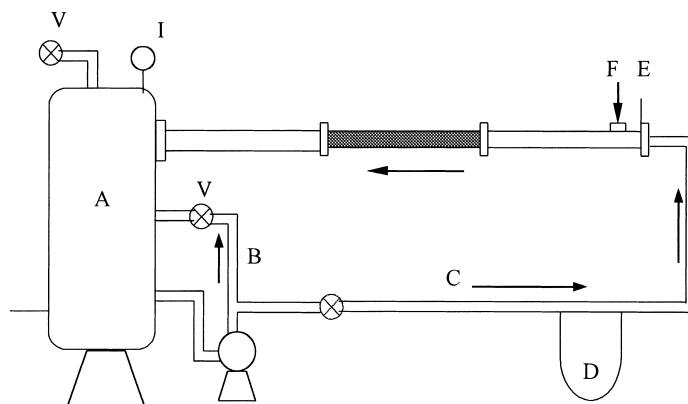
---

\* Corresponding author. Tel.: +1-740-593-9922; fax: +1-740-593-9949.

*E-mail address:* thong@bobcat.ent.ohiou.edu (T. Hong).

to be transported as a mixture of oil, saltwater and gas to the remote separating and refining facilities. Transporting the multiphase mixture makes the corrosion problems even worse. There are many flow regimes depending on the different flow rate of liquid and gas. At the high product rate, the slug flow regime is prominent. Slug flow is known to severely enhance internal corrosion in pipelines due to the mixing vortex and bubble impact in the mixing zone of slug [1,2]. Slug flow is characterized by a dimensionless Froude number ( $Fr$ ) [3]. The turbulence levels and bubble impact on the pipe wall increase with the increase in Froude number. The high rate of wall shear stress due to the turbulence and bubble impact can reduce the performance of inhibitors that might have otherwise formed on the pipe wall [2].

Although the imidazoline-based corrosion inhibitors are widely used by oil industries, very little is understood about their performance under multiphase flow conditions. Most of the studies on the inhibition mechanisms of imidazoline-based inhibitors were conducted in laboratory scale systems, such as the Rotating Cylinder Electrode cell or the laboratory scale flow loop [4–10]. Inability to predict the effects of multiphase flow patterns on inhibitors can seriously degrade the inhibition effectiveness of inhibitors [11]. This work is conducted for studying the inhibition performance of an imidazoline-based inhibitor formulated with the commercial grade imidazoline and dimer–trimer acid under multiphase flow conditions using the EIS technique. The experimental results of this corrosion inhibitor under multiphase flow conditions are discussed.



- |                                     |                   |
|-------------------------------------|-------------------|
| A. Liquid tank                      | G. Test section   |
| B. Bypass                           | H. Gas outlet     |
| C. Liquid feed                      | I. Pressure gauge |
| D. Orifice plate with mercury meter | K. Heater         |
| E. Flow height control gate         | V. Valves         |
| F. Gas input                        |                   |

Fig. 1. Experimental system.

## 2. Experimental

Experiments were carried out in a 101.6 mm I.D., 15 m long acrylic pipeline. The schematic layout of the system is shown in Fig. 1. The detailed description of this system has been reported [1]. The liquid is forced under gate E into the 101.6 mm I.D. Plexiglas pipe, where it forms a fast moving liquid film. The carbon dioxide gas is also introduced into the system at port F. The gas/liquid mixture passes through the Plexiglas pipeline. All the measurements are taken in the test section G located 8 m downstream from the gate. This system can generate two-flow conditions. They are full pipe flow and stationary slug flow. Full pipe flow is a flow pattern with a single liquid phase flowing along the flow loop without feeding gas. The flow rate of liquid phase is controlled by a bypass line B and is measured by a calibrated orifice meter D. For the slug flow experiments, a hydraulic jump [1] is generated and moved into the test section by controlling the gas flow at the inlet F under a certain liquid flow rate.

Studies are carried out using the ASTM substitute saltwater and carbon dioxide gas. The system temperature and pressure are maintained constant at 40°C and 0.136 MPa, respectively, for all experiments. The pH value of the saltwater solution is about 5.6 and the conductivity of saltwater is around  $0.046 \Omega^{-1} \text{ cm}^{-1}$ . The inhibitor used in this work is an imidazoline-based inhibitor formulated with the commercial grade imidazoline and dimer–trimer acid. Imidazoline is the active ingredient of the inhibitor package and its molecular structure is presented as

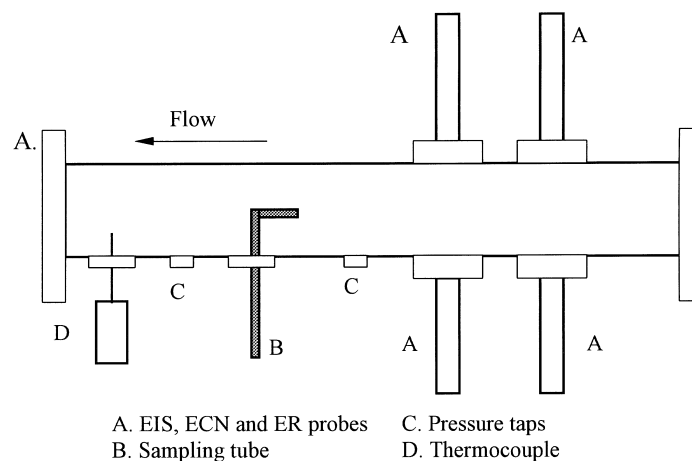
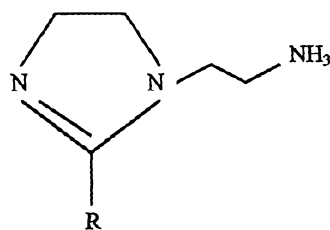


Fig. 2. Test section.



**R = C<sub>16</sub> – C<sub>18</sub> chain**

Imidazoline-based inhibitors inhibit corrosion by blocking the area of metal surface by the adsorbed inhibitor film [12]. The imidazoline molecule bonds with the metal surface by the five-member ring structure containing two nitrogen atoms, which are loaded with electrical charges that make the ring hydrophilic, leaving the long hydrocarbon tail above the surface [6,7,12]. This forms a hydrophobic barrier to water molecules and active species. The most probable configuration of the imidazoline ring is parallel to the metal surface so that the hydrophobic aliphatic chain extends into the solution [6,7]. Optical polarization studies have confirmed that the imidazoline molecules are flat on the surface [13]. The inhibitor concentrations of 25 and 100 ppm are used in this work.

The EIS probe is inserted into the test section G as shown in Fig. 2, and is flush mounted with the pipe wall. A three-electrode arrangement is used in this work. The working electrode is made of C-1018 carbon steel. The counter and reference electrodes are made of 316L stainless steel. The chemical compositions of C-1018 carbon steel and 316L stainless steel are presented in Tables 1 and 2, respectively. The surface area of each electrode is 0.785 cm<sup>2</sup> (diameter is 10 mm). The distance between the centers of each electrode is about 13 mm as shown in Fig. 3.

Preliminary studies were made in a RCE system. The test was carried out in carbon dioxide-saturated ASTM saltwater at a constant temperature of 40°C and stirring speed 1000 rpm. The counter electrodes (CE) are two graphite rods, the reference electrode (RE) is a Saturated Calomel Electrode (SCE) and the working electrode (WE) is 316L stainless steel with a surface area of 3.02 cm<sup>2</sup>. Fig. 4 shows the steady open circuit potential of the stainless steel immersed in carbon dioxide-saturated ASTM saltwater for over 3 h. This figure shows that 316L stainless steel is suitable for being the reference electrode in the test solution used in this work.

Once the de-oxygenation process is complete, the EIS probe, which is first polished by 600-rid sandpaper then rinsed with acetone and distilled water for several times, is inserted into the test section and the EIS measurement started.

Table 1  
Chemical composition of type C-1018 carbon steel (wt%)

C	Si	P	S	Mn	Al	Fe
0.21	0.38	0.09	0.05	0.05	0.01	Balance

Table 2  
Chemical composition of type 316L stainless steel (wt%)

C	Si	Ni	S	Mn	Mo	Cr	Fe
0.02	0.80	14.00	0.02	1.10	2.00	17.00	Balance

The AC impedance spectra in this work is generated by Gamry CMS300 corrosion monitoring system and analyzed using the accompanying software. The EIS measurements are carried out at the open circuit potential with an amplitude of 10 mV AC potential in the frequency range of 20 mHz to 5 kHz. Full pipe flow is studied for liquid velocity of 1.25 m/s and slug flow for Froude number 9. For the inhibition experiments, the inhibitor is injected into the flow loop system and fully mixed with the test solution before the EIS probe is installed into the system.

### 3. Results and discussion

Fig. 5 shows the comparison of experimental results for C-1018 carbon steel exposed to carbon dioxide-saturated ASTM saltwater between the blank test and inhibition test at the inhibitor concentration of 100 ppm for 5 h under 1.25 m/s full pipe flow. The EIS measurement for the inhibition test is conducted at the open circuit potential with an amplitude of 10 mV AC potential in the frequency range of 5 mHz to 5 kHz. As shown in Fig. 5(a), the Nyquist plot for the inhibition test presents one depressed semicircle with a long tail at the low frequency region, while only one depressed semicircle for the blank test. The tail is inclined at an angle of  $45^\circ$  to the Real-axis at very low frequency (Bode phase angle plots also present that the phase angle at very low frequency for the inhibition test decreases approaching to  $-45^\circ$ ). This behavior indicates that the diffusion process of ions takes place on the electrode after the addition of

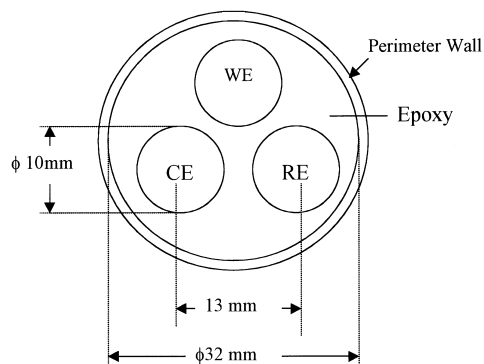


Fig. 3. EIS probe used in the flow loop system.

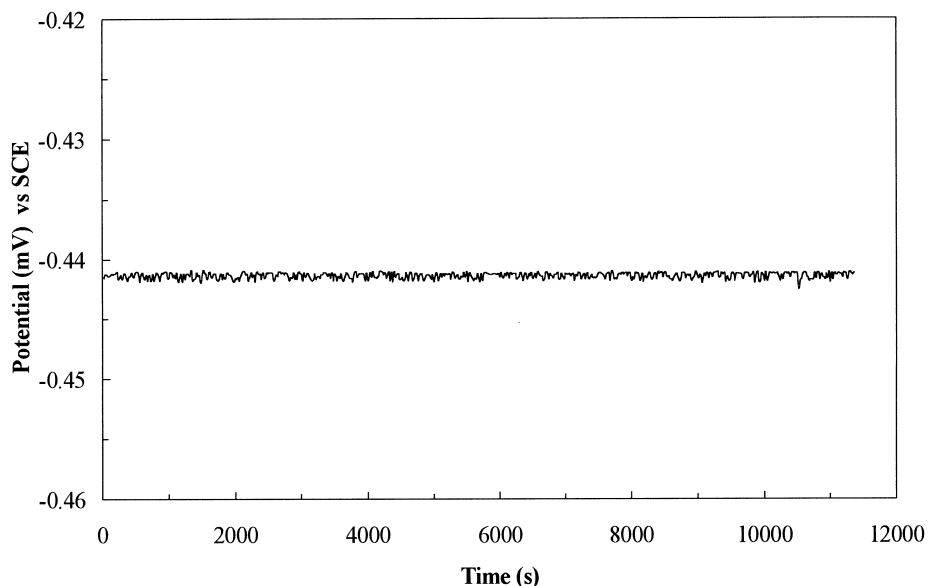


Fig. 4. Open circuit potential versus time for 316L stainless steel exposed to CO<sub>2</sub>-saturated ASTM saltwater in the RCE system.

corrosion inhibitor. On the other hand, it can be observed that the diameter of semicircle for the inhibition test is much larger than the blank test. The corresponding Bode impedance plots as shown in Fig. 5(b) also show that the impedance value in the presence of inhibitor is larger than the blank test. These mean that the corrosion rate is reduced in the presence of the corrosion inhibitor.

There are two methods to describe the EIS spectra for the inhomogeneous films on the metal surface or rough and porous electrodes. One is the finite transmission line model [14]. The other is the filmed equivalent circuit model, which is usually proposed to study the degradation of coated metals [15,16]. It has been suggested that the EIS spectra for the metal covered by organic inhibitor films are very similar to the failed coating metals [17]. Therefore, in this work the filmed equivalent circuit model is used to describe the inhibitors-covered metal/solution interface under flow conditions.

The standard circuit model for coating metals/solution interface used extensively in the literature is shown in Fig. 6(a) [15,16]. Here,  $R_s$  is the solution resistance,  $R_f$  and  $C_f$  are the coating film resistance and capacitance, respectively.  $R_t$  is the charge transfer resistance,  $C_{dl}$  is the double layer capacitance that characterizes the charge separation between metal and electrolyte interface and  $Z_w$  is the Warburg impedance.  $Z_w$  can be presented as [18]

$$Z_w = \sigma \omega^{-1/2} (1 - j) \quad (1)$$

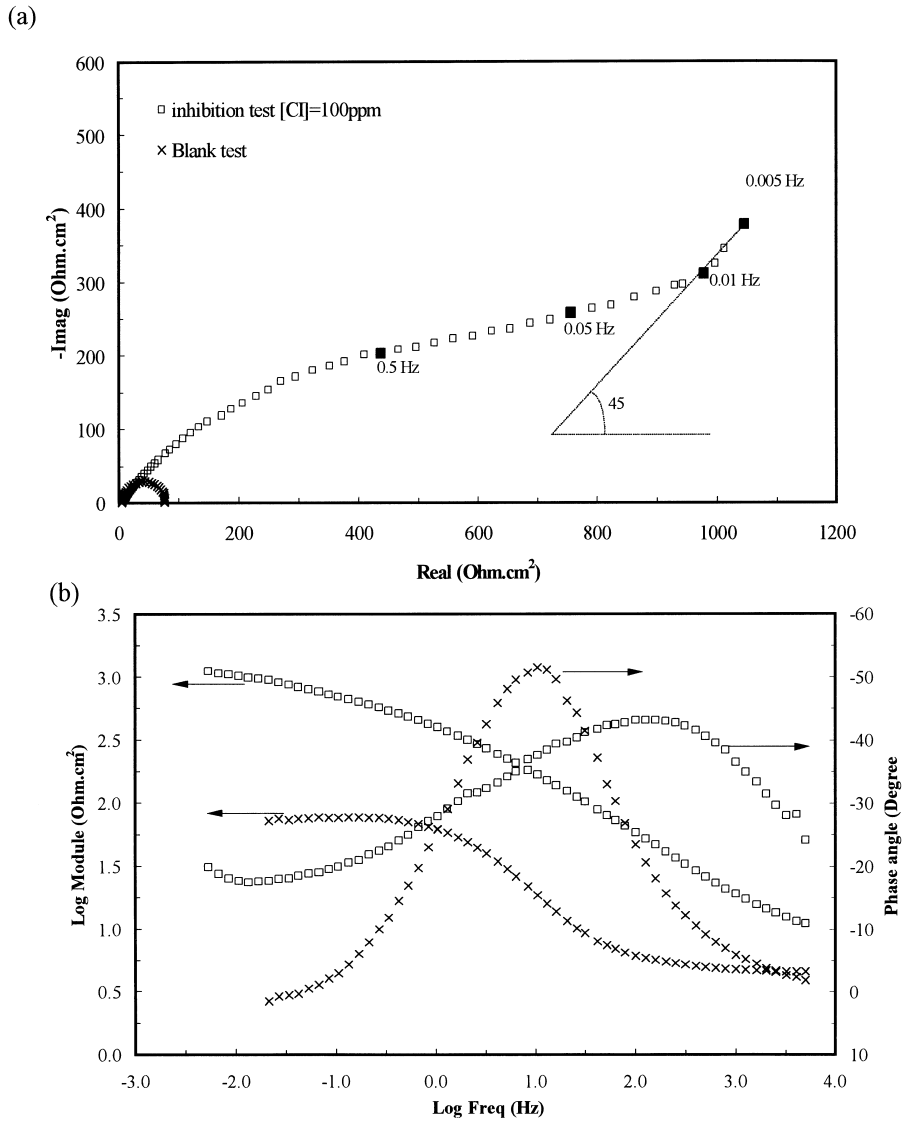


Fig. 5. EIS spectra of carbon steel for the blank test and inhibition test at the concentration of 100 ppm in ASTM saltwater 1.25 m/s full pipe flow. (a) Nyquist plot; (b) Bode plots.

where,  $\sigma$  is the Warburg coefficient ( $\Omega \text{ cm}^2 \text{ s}^{-1/2}$ );

$$\omega = 2\pi f \quad (\text{rad s}^{-1}).$$

The model as shown in Fig. 6(a) includes two parallel resistance and capacitance combinations and Warburg impedance, which are considered to contain coating

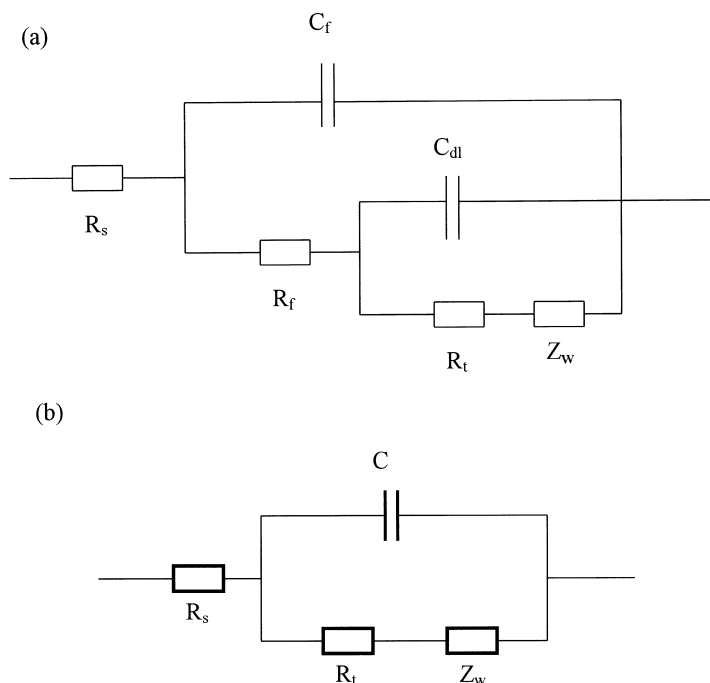


Fig. 6. (a) Equivalent circuit model for interpreting the coating metal.  $R_s$ , solution resistance;  $R_f$ , coating film resistance;  $C_f$ , coating film capacitance;  $R_t$ , charge transfer resistance;  $C_{dl}$ , double layer capacitance;  $Z_w$ , Wargurg impedance. (b) Simplified equivalent circuit model for the metal covered by porous inhibitor films.

film, metal substrate and diffusion information [15,16]. Two semicircles and a diffusion tail would be expected on the Nyquist plot. However, it is difficult to find two semicircles for C-1018 carbon steel exposed to the inhibitor containing solution in Fig. 5(a). This could result from the fact imidazoline adsorbed on the metal surface forms a monolayer [6,12], and the high rate of wall shear stress of the turbulent flow makes the inhibitor film porous. It can be considered that the inhibitor film resistance ( $R_f$ ) is much smaller than the charge transfer resistance ( $R_t$ ). The semicircle representing the inhibitor film merges with the charge transfer loop [18]. Hence, the EIS spectra for the inhibition test as shown in Fig. 5 are described by a simple equivalent circuit as shown in Fig. 6(b).

At low frequency, the capacitive component  $C$  ( $C = C_f + C_{dl}$ ) no longer affects the total impedance value and the total impedance,  $Z_t$ , can be presented as [19]

$$Z_t = R_s + R_t + \sigma\omega^{-1/2} - \sigma\omega^{-1/2}j. \quad (2)$$

From Eq. (2), the imaginary portion,  $-\sigma\omega^{-1/2}j$ , only represents the information of diffusion process. Therefore, in the Nyquist plot at low frequency, where the diffusion tail shows up, the value of Imag-axis presents the item of  $\sigma\omega^{-1/2}$ . The

modulus of Warburg impedance  $|Z_w| = \sqrt{2\sigma\omega}^{-1/2}$ , so that Warburg impedance can be obtained by the value of Imag-axis at low frequency. Here,  $b_f$ , which is defined as following equation, is qualitatively represented as the Warburg impedance.

$$b_f = -\sigma\omega^{-1/2} \quad (3)$$

The steel surface covered by porous inhibitor film can be represented by Fig. 7. The larger the value of  $b_f$ , more difficult for the ions to diffuse through the pores within the inhibitor films. The larger  $b_f$  might indicate that the inhibitor films are less porous or have pores with smaller equivalent diameter. The following experimental results of the inhibitor tests in the flow loop will be discussed by the value of  $b_f$ .

It takes a long time (over 1 h) to conduct the measurement using as low frequency as 5 mHz. Since a large amount of gas is used to generate slugs, it is not suitable to take the EIS measurements at very low frequency (e.g. 5 mHz) in the slug flow condition. Hence, most of the experiments were conducted at the frequency range of 20 mHz to 5 kHz. Fig. 8 shows is the Nyquist plots for C-1018 carbon steel at different exposure times in ASTM saltwater with 25 ppm inhibitor under slug flow at Froude number 9. The diameter of the semicircle increases with time, which means that the charge transfer resistance increases with time. This results from the fact that the corrosion rate decreases with exposure time in the inhibitor containing solution. The diffusion tail is observed for all the exposure times. The value of  $b_f$  corresponding to the low frequency of 0.068 Hz increases with exposure time. This fact implies that the inhibitor films adsorbed on the metal surface become less porous with time and lead to the reduction of the corrosion rate with time.

Fig. 9 shows the Nyquist plots of C-1018 carbon steel in the saltwater with 100 and 25 ppm inhibitor under Froude number 9 slug flow at the same exposure time

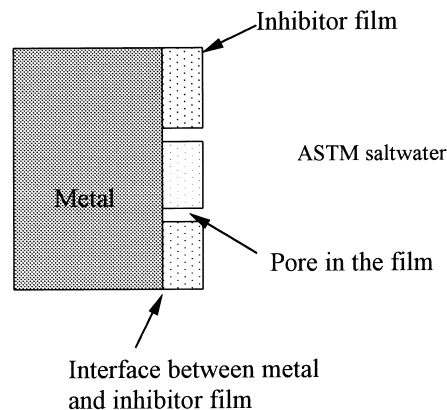


Fig. 7. A schematic diagram of the metal covered by porous inhibitor films.

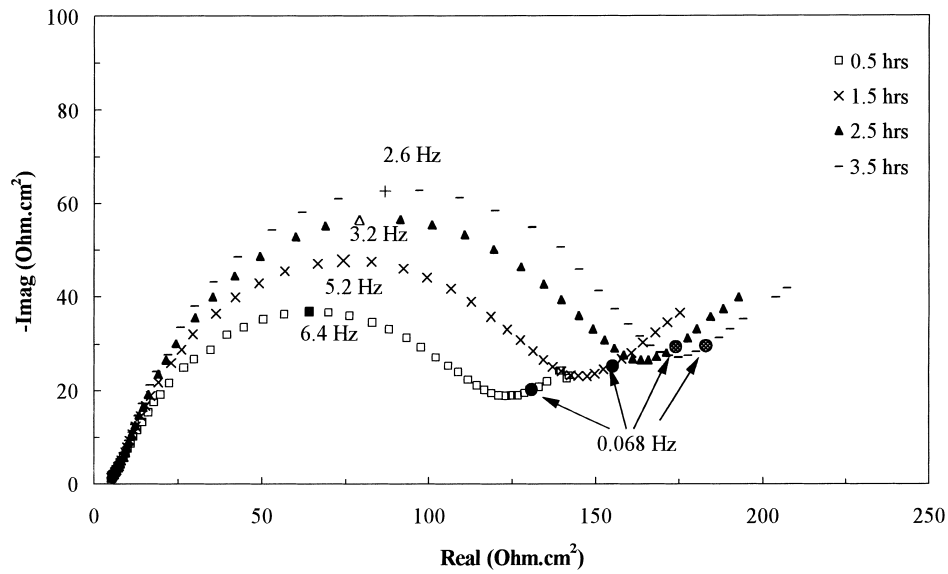


Fig. 8. Nyquist plot of carbon steel in ASTM saltwater with 25 ppm inhibitor under Froude number 9 slug flow at different exposure times.

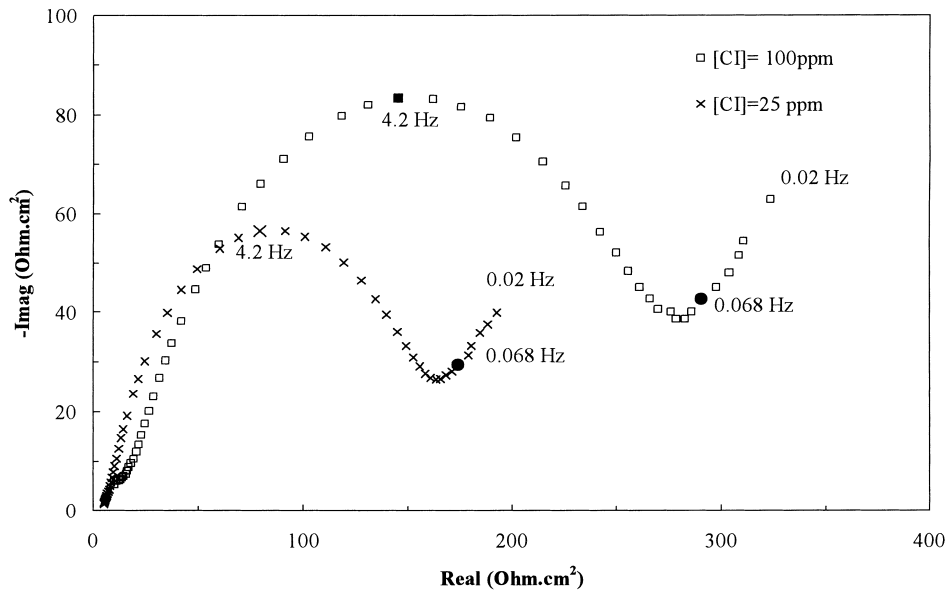


Fig. 9. Nyquist plot of carbon steel in ASTM saltwater with different concentrations of inhibitor under Froude number 9 slug flow at exposure time 2.5 h.

of 2.5 h. The value of  $b_f$  for 100 ppm inhibitor is larger than 25 ppm at a low frequency of 0.068 Hz. This could indicate that inhibitor films are less porous at higher inhibitor concentration. Also, the charge transfer resistance at 100 ppm inhibitor concentration is larger than 25 ppm. This means that the corrosion rate becomes lower at higher inhibitor concentration. These demonstrate that this corrosion inhibitor has a good performance of corrosion protection by forming more compact inhibitor films on the metal surface at the higher inhibitor concentration.

Fig. 10 presents the comparison of EIS spectra for C-1018 carbon steel in ASTM saltwater with 25 ppm inhibitor under different flow conditions. It can be seen that the charge transfer resistance for slug flow at Froude number 9 has a smaller value than 1.25 m/s full pipe flow. Again, the value of  $b_f$  corresponding to the frequency of 0.068 Hz in the diffusion region for slug flow is lower than full pipe flow. This result indicates that the performance of the inhibitor is affected by the flow conditions. In the turbulent slug flow, there is a highly frothy turbulent region. The gas in this region is in the form of pulse of bubbles. These bubbles are trapped by the mixing vortex and shot to the bottom of the pipe where they can impact and collapse on the pipe walls [1]. Some inhibitor films, which have been adsorbed on the metal surface, are damaged by the turbulence and bubble impact and washed away from there. Hence, the inhibitor films in slug flow are more porous than in full pipe flow, leading to a higher corrosion rate under multiphase turbulent slug flow conditions.

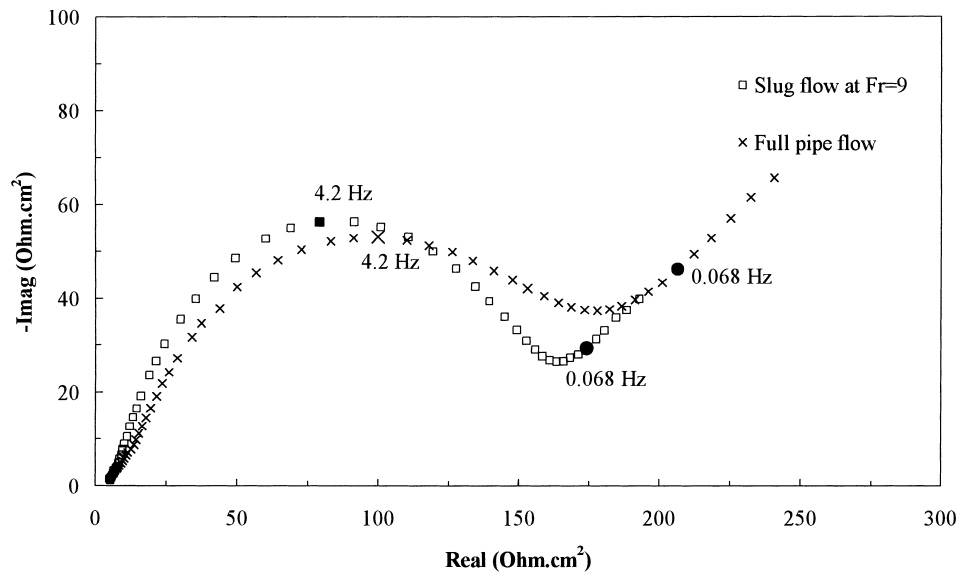


Fig. 10. Nyquist plot of carbon steel in ASTM saltwater with 25 ppm inhibitor under different flow conditions at exposure time 3.5 h.

#### 4. Conclusions

This work presented here shows that the EIS technique is a good method to study the inhibition performance of corrosion inhibitors under multiphase flow conditions. The Warburg parameter,  $b_f$ , can be used to qualitatively study the inhibition performance of inhibitor films formed on the metal surface.

Experimental results show that the inhibitor film is correlated to the exposure time and inhibitor concentration. The film becomes less porous with the increase of exposure time and concentration. The turbulent flow at the high rate of turbulence and bubble impact can degrade the inhibitor performance and increase the corrosion rates. This work shows that one of the critical criteria to select inhibitors used for oil and gas pipelines is whether the inhibitors have a good performance under actual flow conditions.

#### References

- [1] Jyi-Yu Sun, W.P. Jepson, SPE Paper 24787 (1992) 215.
- [2] A.S. Green, B.V. Johnson, H. Choi, SPE Paper 20685 (1989) 677.
- [3] W.P. Jepson, in: 3rd Int. Conf. on Multiphase Flow, The Hague, Netherlands, 1987, p. 187.
- [4] Y.J. Tan, S. Bailey, B. Kinsella, Corrosion Science 38 (10) (1996) 1681.
- [5] Y.J. Tan, S. Bailey, B. Kinsella, Corrosion Science 38 (9) (1996) 1545.
- [6] D. Klenerman, J. Hodge, M. Joseph, Corrosion Science 36 (2) (1994) 301.
- [7] A. Edwards, C. Osborne, S. Webster, et al., Corrosion Science 36 (2) (1994) 315.
- [8] C. Neice, G.T. Solvi, S. Skjerve, British Corrosion Journal 32 (4) (1997) 269.
- [9] Y.J. Tan, B. Kinsella, S. Bailey, British Corrosion Journal 32 (3) (1997) 212.
- [10] S. Bailey, Y.J. Tan, B. Kinsella, British Corrosion Journal 32 (1) (1997) 49.
- [11] H.J. Choi, R.L. Cepulis, SPE Production Engineering (11) (1987) 325.
- [12] S. Ramachandran, B.L. Tsai Jr, M. Blanco, et al., Langmuir 12 (26) (1996) 6419.
- [13] A.J. Mc Mahon, Collids Surf 59 (1991) 187.
- [14] J.R. Park, D.D. Macdonald, Corrosion Science 23 (4) (1983) 295.
- [15] G.W. Walter, Corrosion Science 32 (10) (1991) 1041.
- [16] G.W. Walter, Corrosion Science 30 (6/7) (1990) 617.
- [17] F. Mansfeld, Electrochemica Acta 35 (10) (1990) 1533.
- [18] G.W. Walter, Corrosion Science 26 (9) (1986) 681.
- [19] T. Hong, G.W. Walter, M. Nagumo, Corrosion Science 38 (9) (1996) 1525.